Ab initio calculations of one-electron-scattering properties of methane

Per Kaijser
Siemens AG, Communication and Information Systems, Otto-Hahn-Ring 6, Postfach 830951, D-8000 Munchen 83, Federal Republic of Germany

Vedene H. Smith, Jr. and A. N. Tripathi*
Department of Chemistry, Queen's University, Kingston, Ontario, Canada K7L 3N6

Geerd H. F. Diercksen
Max-Planck-Institut für Physik und Astrophysik, Institut für Astrophysik, D-8046 Garching (Munchen), Federal Republic of Germany

(Received 3 November 1986)

Directional x-ray scattering factors and Compton profiles have been evaluated in several directions relevant to the molecular structure of CH_4 and compared to their respective isotropic components for four different self-consistent-field wave functions and one single-determinant configuration-interaction wave function constructed especially for this study with Cartesian Gaussian-type basis orbitals. The internally folded density ("reciprocal form factor") $B(\mathbf{r})$ is calculated and discussed as are various momentum-space expectation values. A comparison is made with available experimental and other theoretical results.

I. INTRODUCTION

Because of the interest in measuring one-electron-scattering properties (e.g., Compton profiles and elastic scattering intensities), it is important to assess the accuracy of the calculated quantities. In this paper we study the isotropic components of these one-electron-scattering quantities, as well as their components in various directions for the case of methane. Although the current methods of measurement of directional properties are restricted to solids, single crystals, or largely layered materials such as graphite, we have calculated the directional properties because they reveal much more information about the electronic structure.

The elastic or coherent x-ray scattering intensity is proportional to the modulus squared of the scattering factor $F(\mathbf{s})$, where $\mathbf{s}$ is the scattering vector. $F(\mathbf{s})$ is related to the electron density in position space $\rho(\mathbf{r})=\gamma(\mathbf{r},\mathbf{r})$ by a three-dimensional Fourier transformation[1,2]

$$F(\mathbf{s})=\int \gamma(\mathbf{r},\mathbf{r})e^{i\mathbf{s}\cdot\mathbf{r}}d\mathbf{r}\ , \tag{1}$$

where $\gamma(\mathbf{r},\mathbf{r}')$ is the position-space representation of the spin-traced one-electron reduced density matrix defined by

$$\gamma(\mathbf{r},\mathbf{r}')=N\int \psi^*(\mathbf{r}'\sigma,\mathbf{x}_2,\mathbf{x}_3,\cdots,\mathbf{x}_N)\times\psi(\mathbf{r}\sigma,\mathbf{x}_2,\mathbf{x}_3,\cdots,\mathbf{x}_N)d\sigma\, d\mathbf{x}_2 d\mathbf{x}_3\cdots d\mathbf{x}_N\ , \tag{2}$$

ψ is the position-space representation of the N-electron wave function and $\mathbf{x}_i=(\mathbf{r}_i,\sigma_i)$ is a combined space-spin coordinate for electron i.

In the gas phase, the measured quantity is the isotropic component of $|F(\mathbf{s})|^2$, i.e.,

$$I_{\rm el}^{\rm xr}/I_T=\frac{1}{4\pi}\int |F(\mathbf{s})|^2 d\Omega_s\ . \tag{3}$$

This relation in general corresponds to the situation where the rotational energy differences are not resolved. However, if they are resolved, then a fully elastic x-ray intensity from the $J=0$ state[3,4] can be extracted from the knowledge of the scattering factor $F(\mathbf{s})$, i.e.,

$$I_{\rm fel}^{\rm xr}/I_T=\left|\frac{1}{4\pi}\int F(\mathbf{s})d\Omega_{\rm s}\right|^2\ . \tag{4}$$

The elastic intensities bound the fully elastic ones, i.e.,

$$I_{\rm el}^{\rm xr}(s)\geqq I_{\rm fel}^{\rm xr}(s) \tag{5}$$

with equality holding in the case that $F(\mathbf{s})$ is spherically symmetric.[4] Recently, calculations have been carried out of elastic and total x-ray intensities for some small- to medium-size molecular systems. (See, for example, the recent review by Tripathi and Smith.[5])

The inelastic or incoherent x-ray scattering involves a momentum transfer that broadens the Compton line.[6] The form of this line, the Compton profile, is related to the electron density in momentum space $\Pi(\mathbf{p})$ and is denoted by $J(\mathbf{q})$. Within the impulse approximation[6] the expression for the directional Compton profile (DCP) is[7]

$$J(\mathbf{q})=J(q,\hat{\mathbf{q}})=\int \Pi(\mathbf{p})\delta(\mathbf{p}\cdot\hat{\mathbf{q}}-q)d\mathbf{p}\ , \tag{6}$$

where $\hat{\mathbf{q}}$ is a unit vector along the scattering vector. The spherically averaged or isotropic Compton profile (ICP) is the spherical average of the DCP and is related to the spherically averaged momentum density $\overline{\Pi}(\mathbf{p})$, i.e.,

$$\bar{J}(q)=(4\pi)^{-1}\int_{|\mathbf{q}|=q} J(\mathbf{q})d\Omega_{\hat{\mathbf{q}}}=2\pi\int_q^\infty p\overline{\Pi}(p)dp\ , \tag{7}$$

where

$$\overline{\Pi}(p)=(4\pi)^{-1}\int \Pi(\mathbf{p})d\Omega_{\hat{\mathbf{p}}} . \quad (8)$$

The momentum density $\Pi(\mathbf{p})$ is related by means of a double Fourier transformation[1] to the position-space density matrix $\gamma(\mathbf{r},\mathbf{r}')$ defined in Eq. (2),

$$\Pi(\mathbf{p})=(2\pi)^{-3}\int e^{-i\mathbf{p}\cdot(\mathbf{r}-\mathbf{r}')}\gamma(\mathbf{r},\mathbf{r}')d\mathbf{r}\,d\mathbf{r}' . \quad (9)$$

A useful representation can be obtained by the Fourier transformation of the momentum density,[8-10] i.e.,

$$B(\mathbf{r})=\int e^{-i\mathbf{p}\cdot\mathbf{r}}\Pi(\mathbf{p})d\mathbf{p}=\int \gamma(\mathbf{s},\mathbf{r}+\mathbf{s})d\mathbf{s} . \quad (10)$$

This position-space function is referred to as the internally folded density, the characteristic function of the momentum density, reciprocal form factor, or simply as the $B(\mathbf{r})$ function.

The earliest calculations of momentum-space properties and Compton profiles for molecular methane were made in 1941 by Coulson and Duncanson.[11] Other Compton profile calculations on this molecule have been made by Cornille and co-workers,[12] Epstein,[13] Smith and co-workers,[14] and by Ahlenius and Lindner.[15,16] These reports all dealt with the isotropic Compton profile.

For a general description of the theory, the reader is referred to reviews on these topics[1,2,5,6,17,18] and similarly for the calculational procedures.[7,19] The particular methods used in this paper will be described in detail elsewhere.[20] The calculations were made with the Kingston suite of programs for scattering properties. Atomic units are used throughout this paper unless otherwise explicitly mentioned.[21]

II. WAVE FUNCTIONS

The Hartree-Fock (HF) equations were solved self-consistently (SCF) using the molecular program system MUNICH developed by Diercksen and Kraemer.[22] Cartesian Gaussian-type orbitals (GTO's) were used as the basis functions for the expansion of the molecular orbitals. Table I describes these basis sets, both in terms of the number of primitive and contracted orbitals and the original sources.[23-25] As identification of the wave function we use the number of primitive orbitals on the carbon atom. Thus the (11.7.1) wave function means that there were 11 s-type, 7 p-type, and 1 d-type primitive GTO's on the carbon atom.

The four basis sets in our study may be characterized as "single-ζ [Slater-type orbital represented by three Gaussians (STO-3G)]" (6.3), "improved double-ζ" (11.7), "improved double-ζ plus polarization" (11.7.1), and "improved triple-ζ plus polarization" (13.8.2) basis sets. The SCF (11.7.1) wave function was further extended to a configuration-interaction (CI) calculation by means of the program MOLECULE.[26] In this calculation the carbon core orbitals were kept frozen and all singly and doubly substituted determinants which can be generated within the valence molecular orbital basis from the single-determinant reference state were included. It will be designated as an SDCI wave function. All calculations were performed at the experimental geometry[27] with a C—H bondlength of 1.0935 Å (=2.0665 a.u.).

TABLE I. The number of primitive and contracted Gaussian-type basis orbitals for the carbon and hydrogen atoms.

Notation	Carbon	Hydrogen	Reference
SCF (6.3)	(6.3)/[2.1]	(3)/[1]	25
SCF (11.7)	(11.7)/[5.4]	(6)/[3]	23
SCF, SDCI (11.7.1)	(11.7.1)/[5.4.1]	(6.1)/[3.1]	23
SCF (13.8.2)	(13.8.2)/[7.5.2]	(8.2)/[4.2]	24

III. ENERGIES AND MOMENTUM EXPECTATION VALUES

On the grounds of variational theory, the quality of wave functions has been traditionally determined by the total energy, the average of the Hamiltonian over the wave function. The lower the energy, the better the quality, and we retain this concept despite the fact that for properties other than the total energy it may be quite misleading.[28] In Table II the energies (E) from the present calculations are tabulated. As expected, the "quality" improves with the extension of the basis sets in the SCF calculations and, of course, improves when correlation is taken into account for a given basis set.

The SCF and SDCI wave functions of Kowaleski *et al.*[29] used by Ahlenius and Lindner[15,16] are similar but slightly better energetically than our (11.7.1) wave functions, i.e., −40.2098 hartree (SCF) and −40.4096 hartree (SDCI). They also used Cartesian Gaussian-type basis orbitals (11.7.1)/[5.3.1] for the carbon and (5.1.)/[3.1] for the hydrogen atoms (where the square brackets represent contracted orbitals). Their bases are of the same primitive size as our (11.7.1) but differ slightly in the contractions.

Smith and Whangbo[14] also used Cartesian Gaussian-type basis orbitals in their wave function. They did not include any polarization orbitals in their set C(13.7)/[4.2] and H(4)/[2], for which they obtained the energy −40.1860 hartree, which is slightly better than for our SCF (11.7) wave function.

A minimal basis of Slater-type orbitals was used in Pitzer's wave function[30] which was employed by Epstein in his work.[13] With a total energy of −40.1282 hartree this wave function is considerably better than the single-ζ (STO-3G) one but poorer than a wave function with a set of contracted Gaussian-type orbitals corresponding to a double-ζ basis, i.e., the (11.7).

Hence we observe that the quality, based on the total energy of the wave functions, in the present paper on the SCF level, go beyond what has previously been reported in the literature on Compton profiles. Our SDCI wave function is comparable with that used by Ahlenius and Lindner.[15]

Besides the total energy, the moments of the electron momentum density

$$\langle p^n\rangle=4\pi\int_0^\infty p^{n+2}\overline{\Pi}(p)\,dp \quad (11)$$

were evaluated for the allowed integer values $n=0,\pm1,\pm2,+3,+4$. The values for $n=0$ (not included in Table II) give the number of electrons for methane which was correct to seven digits in our calculations. The factor $\frac{1}{2}$ is introduced for convenience in the table for

TABLE II. The momentum density at the origin, the total energy, and some momentum moments calculated from our five different wave functions. All numbers are in atomic units.

Wave function	$\overline{\Pi}(0)$	$\langle p^{-2}\rangle$	$\frac{1}{2}\langle p^{-1}\rangle$	$\langle p\rangle$	$\frac{1}{2}\langle p^{2}\rangle$	$\langle p^{3}\rangle$	$\langle p^{4}\rangle$	$-E$
SCF (6.3)	1.505	17.375	4.952	18.936	39.435	6.1971×10^{3}	7.3626×10^{3}	39.7265
SCF (11.7)	1.472	17.939	5.057	18.811	40.163	6.9024×10^{3}	1.1348×10^{4}	40.1832
SCF (11.7.1)	1.463	17.891	5.050	18.824	40.134	6.8937×10^{3}	1.1341×10^{4}	40.2078
SDCI (11.7.1)	1.465	17.814	5.026	18.936	40.367	6.9143×10^{3}	1.1356×10^{4}	40.3889
SCF (13.8.2)	1.399	17.747	5.046	18.832	40.143	6.8979×10^{3}	1.1550×10^{4}	40.2153

$n=-1$ and 2 in order to reproduce the peak of the isotropic Compton profile, $J(0)$, and the kinetic energy T, respectively. The latter quantity should be compared with the total energy for judgment of the quality of the geometric configuration. At the true equilibrium geometry, the kinetic energy T equals $-E$ according to the virial theorem.[31] The value of the $\langle p^4\rangle$ moments determines the quasirelativistic correction (Breit-Pauli) to the kinetic energy due to the variation of electron mass with velocity.[32]

Epstein[13] evaluated several momentum moments for the Pitzer wave function (minimal basis of Slater-type orbitals). The results were in order ($n=-2$, -1, 1, and 2), 18.37, 5.045, 18.92, and 40.145, respectively, which with the exception of $\langle p^{-2}\rangle$ are very similar to those of the SCF (13.8.2), in spite of the rather large difference in total energy.

The probability of finding an electron at rest, i.e., the momentum density at the origin $\overline{\Pi}(0)$, is included in Table II. For Slater-type orbitals only s orbitals contribute to $\overline{\Pi}(0)$.[7,33] This is also true for Cartesian Gaussian-type orbitals if the prefactor of the exponential is in the form of a Hermite polynomial.[7] In the present wave functions the prefactors of the d-type Cartesian GTO's are x^2, y^2, z^2, xy, yz, and xz in position space and they will contribute[7] to $\overline{\Pi}(0)$. The effect of inclusion of these polarization functions is to slightly reduce $\overline{\Pi}(0)$, i.e., they decrease the occupancy of diffuse s orbitals.

The reason why the correlation effect on $\overline{\Pi}(0)$ is so small is mainly due to the frozen-core approximation, i.e., the carbon core orbitals did not take part in the CI calculations. Therefore, due to orthogonality constraints, only minor changes to the $\overline{\Pi}(0)$ contributing orbitals occurred.

We note that correlation lowers the negative power moments ($n=-1,-2$) and increases all the positive power moments ($n=1,2,3,4$). This behavior is consistent with the intuitive expectations[34,35] based on the virial theorem[31] that the decrease (increase) in total (kinetic) energy due to electron correlation should lead to a correlated momentum distribution which is more diffuse than the HF one.

IV. RESULTS AND DISCUSSION OF DIRECTIONAL SCATTERING PROPERTIES

For the three directions illustrated in Fig. 1 we evaluated the scattering factors $F(\mathbf{s})$ and the directional Compton profiles $J(\mathbf{q})$. The arrows 1, 2, and 3 indicate the directions along which the vectors $\mathbf{s}$ and $\mathbf{q}$ are aligned. All three directions lie in a plane containing the carbon nucleus and two of the four protons of the methane molecule. The other two protons are below the carbon nucleus, one in front of and the other behind the plane. Direction 1 bisects the tetrahedral HCH angle while 3 is perpendicular to 1 and 2 lies along a CH bond. It should be noted that for methane there are 6 directions equivalent to 1, 4 directions equivalent to 2, and 12 directions equivalent to 3 in position space. Due to inversion symmetry in momentum space,[36] there are 6, 8, and 12 equivalent directions in momentum space, respectively.

A. Scattering factors

The scattering factors $F(\mathbf{s})$ were evaluated for the five wave functions in each of the three different directions 1, 2, and 3 of $\mathbf{s}$ and are presented in Table III. It is seen that $F(\mathbf{s})$ is essentially independent of the quality of the wave function, not only within the SCF level, but also from correlation.

Directional dependences are, on the other hand, certainly present in $F(\mathbf{s})$. In direction 1, the scattering factor decays the fastest, and in direction 3, the slowest. These results give us information about the charge density projected onto the scattering vector $\mathbf{s}$.[37] Thus the density so projected is most concentrated along direction 3, which is intuitively correct since there exists a plane orthogonal to this direction that contains the carbon atom and two of the four hydrogen atoms. We will return to this point in the discussion.

B. The directional Compton profiles

Directional Compton profiles (DCP) were evaluated with the scattering vector along the same three directions as for $F(\mathbf{s})$ and the results are presented in Table IV as the difference of the DCP from the ICP of the same wave function. The ICP's are given in Table V.

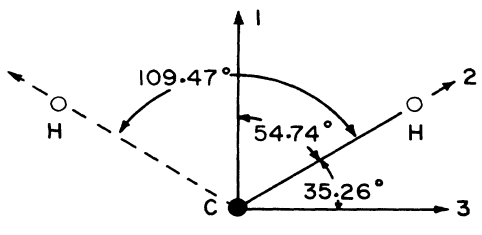

FIG. 1. The three directions (1, 2, and 3) of the scattering vector used in the present study. They are in a plane containing the carbon and two of the four hydrogen nuclei of the methane molecule.

TABLE III. The directional scattering factors per electron for the methane molecule.

	Direction 1					Direction 2					Direction 3				
$\sin(\theta/\lambda)$ (Å^{-1})	SCF (6.3)	SCF (11.7)	SCF (11.7.1)	SDCI (11.7.1)	SCF (13.8.2)	SCF (6.3)	SCF (11.7)	SCF (11.7.1)	SDCI (11.7.1)	SCF (13.8.2)	SCF (6.3)	SCF (11.7)	SCF (11.7.1)	SDCI (11.7.1)	SCF (13.8.2)
0.00	1.000	1.000	1.000	1.000	1.000	1.000	1.000	1.000	1.000	1.000	1.000	1.000	1.000	1.000	1.000
0.02	0.990	0.989	0.989	0.989	0.989	0.990	0.990	0.989	0.989	0.989	0.990	0.989	0.989	0.989	0.989
0.04	0.960	0.958	0.959	0.959	0.959	0.960	0.960	0.959	0.959	0.959	0.960	0.959	0.959	0.959	0.959
0.06	0.912	0.909	0.910	0.910	0.910	0.914	0.910	0.911	0.911	0.911	0.914	0.910	0.911	0.910	0.911
0.08	0.851	0.846	0.847	0.847	0.847	0.854	0.848	0.849	0.849	0.849	0.853	0.847	0.848	0.848	0.849
0.10	0.778	0.771	0.773	0.773	0.774	0.785	0.777	0.779	0.779	0.779	0.783	0.776	0.777	0.777	0.777
0.12	0.699	0.691	0.693	0.693	0.694	0.711	0.703	0.704	0.705	0.705	0.707	0.699	0.701	0.701	0.702
0.14	0.617	0.609	0.612	0.612	0.613	0.638	0.629	0.631	0.631	0.631	0.631	0.622	0.625	0.625	0.625
0.16	0.536	0.528	0.532	0.533	0.533	0.568	0.559	0.561	0.562	0.562	0.557	0.549	0.552	0.552	0.552
0.18	0.459	0.453	0.457	0.458	0.459	0.505	0.497	0.499	0.501	0.499	0.490	0.482	0.484	0.486	0.485
0.20	0.388	0.384	0.389	0.390	0.390	0.451	0.444	0.445	0.447	0.446	0.429	0.423	0.425	0.427	0.426
0.25	0.248	0.250	0.255	0.257	0.256	0.352	0.347	0.348	0.350	0.348	0.316	0.314	0.314	0.317	0.315
0.30	0.161	0.170	0.173	0.175	0.173	0.291	0.286	0.288	0.290	0.289	0.253	0.255	0.252	0.255	0.252
0.40	0.109	0.122	0.119	0.122	0.118	0.210	0.210	0.214	0.214	0.215	0.214	0.216	0.211	0.213	0.212
0.50	0.126	0.134	0.130	0.132	0.129	0.159	0.163	0.166	0.166	0.167	0.201	0.201	0.199	0.200	0.199

First we note that the DCP's depend both on direction and wave-function quality. The highest peak value is for direction 1 and the lowest is for 2.

By combining the ICP and the DCP tables, we find that the slowest decay in the vicinity of the peak occurs when the scattering vector is along a CH bond (direction 2). This is logical, since the DCP along 2 has the lowest peak and the same norm and also since there is a plane close to, but not through, the origin with a considerable amount of momentum density, which is built up from the three bond orbitals, all of which contain some p-orbital character.

The DCP along direction 3 is closer to the ICP than the other two, since on the unit sphere in momentum space there are 12 directions equivalent to it for molecular methane while there are only 6 equivalent to direction 1 and 8 equivalent to direction 2. It is thus expected that the largest deviations from the ICP should occur along direction 1 as inspection of the data in Table IV confirms.

As the SCF wave-function quality improves, the deviations from the ICP decrease indicating a more spherical momentum density. The changes due to correlation affect the DCP's and the ICP by almost the same amount so that the difference between DCP and ICP for the two wave functions (one correlated and one uncorrelated) with the (11.7.1) basis are essentially the same.

C. Discussion

The methane molecule is a good example to illustrate the difference between the electron density in position and in momentum space. The symmetry group T_d to which methane belongs does not obey inversion symmetry. As a consequence, the electron charge density in position space does not obey inversion symmetry either. The electron momentum density does, however, include inversion symmetry irrespective of the symmetry group to which the molecule belongs.[36] It is due to this fact that there are 6, 8, and 12 directions on the unit sphere equivalent to directions 1, 2, and 3, respectively, in momentum space. The corresponding numbers in position space are 6, 4, and 12.

There are many similarities between scattering factors and directional Compton profiles and their relations to the position and momentum electron densities.[8–10] The point which we wish to stress in this paper is the projection of the density onto the scattering vector, i.e., integrating over the density in a plane orthogonal to the scattering vector. In momentum space, this quantity is the directional Compton profile. In position space, this quantity is related to the scattering factor via a one-dimensional Fourier transformation.[8,37] With the use of these concepts one can interpret the momentum density in planes orthogonal to the scattering vector from the DCP's and in a less direct way the charge density in position space in planes orthogonal to the vector $\mathbf{s}$ from $F(\mathbf{s})$.

With this in mind and the knowledge of the properties of one-dimensional Fourier transforms, it is not surprising that $F(\mathbf{s})$ for $\mathbf{s}$ along direction 3 decays the slowest, since there is no plane containing as much density as one orthogonal to this direction. The fastest decaying $F(\mathbf{s})$ is with $\mathbf{s}$ along the direction bisecting a HCH angle (direction 1), since the projected density on this line is the most

TABLE IV. The differences between the three directional Compton profiles and the isotropic Compton profile of the same wave function for the methane molecule.

	Direction 1					Direction 2					Direction 3				
q	SCF	SCF	SCF	SDCI	SCF	SCF	SCF	SCF	SDCI	SCF	SCF	SCF	SCF	SDCI	SCF
(a.u.)	(6.3)	(11.7)	(11.7.1)	(11.7.1)	(13.8.2)	(6.3)	(11.7)	(11.7.1)	(11.7.1)	(13.8.2)	(6.3)	(11.7)	(11.7.1)	(11.7.1)	(13.8.2)
0.0	0.1250	0.1127	0.0975	0.0921	0.0852	−0.1081	−0.1003	−0.0759	−0.0723	−0.0672	−0.0258	−0.0202	−0.0237	−0.0225	−0.0208
0.1	0.1144	0.1017	0.0877	0.0827	0.0766	−0.0998	−0.0916	−0.0690	−0.0657	−0.0615	−0.0232	−0.0177	−0.0210	−0.0199	−0.0179
0.2	0.0856	0.0724	0.0616	0.0579	0.0537	−0.0769	−0.0681	−0.0506	−0.0481	−0.0390	−0.0162	−0.0113	−0.0139	−0.0130	−0.0114
0.3	0.0458	0.0335	0.0273	0.0254	0.0240	−0.0447	−0.0363	−0.0260	−0.0247	−0.0254	−0.0068	−0.0031	−0.0045	−0.0041	−0.0027
0.4	0.0041	−0.0050	−0.0062	−0.0062	−0.0047	−0.0101	−0.0037	−0.0015	0.0014	0.0046	0.0026	0.0045	0.0043	0.0043	0.0053
0.5	−0.0314	−0.0353	−0.0319	−0.0304	−0.0266	0.0206	0.0237	0.0183	0.0174	0.0128	0.0100	0.0098	0.0108	0.0105	0.0107
0.6	−0.0555	−0.0537	−0.0467	−0.0430	−0.0392	0.0432	0.0422	0.0310	0.0294	0.0257	0.0144	0.0122	0.0140	0.0135	0.0138
0.7	−0.0671	−0.0599	−0.0510	−0.0482	−0.0432	0.0559	0.0511	0.0365	0.0347	0.0313	0.0155	0.0118	0.0142	0.0135	0.0122
0.8	−0.0675	−0.0566	−0.0473	−0.0447	−0.0407	0.0596	0.0519	0.0364	0.0348	0.0333	0.0139	0.0095	0.0120	0.0114	0.0096
0.9	−0.0601	−0.0473	−0.0389	−0.0367	−0.0343	0.0562	0.0470	0.0327	0.0314	0.0318	0.0108	0.0063	0.0086	0.0080	0.0061
1.0	−0.0483	−0.0353	−0.0286	−0.0270	−0.0262	0.0482	0.0388	0.0272	0.0263	0.0280	0.0069	0.0031	0.0048	0.0044	0.0027
1.2	−0.0221	−0.0129	−0.0102	−0.0096	−0.0108	0.0270	0.0204	0.0155	0.0152	0.0176	0.0002	−0.0017	−0.0012	−0.0014	−0.0022
1.4	−0.0021	0.0013	0.0010	0.0011	0.0005	0.0079	0.0058	0.0063	0.0061	0.0074	−0.0034	−0.0034	−0.0038	−0.0038	−0.0037
1.6	0.0087	0.0074	0.0058	0.0057	0.0047	−0.0049	−0.0033	0.0000	0.0002	0.0002	−0.0038	−0.0029	−0.0037	−0.0036	−0.0030
1.8	0.0120	0.0087	0.0068	0.0067	0.0064	−0.0109	−0.0078	−0.0041	−0.0042	−0.0047	−0.0025	−0.0015	−0.0022	−0.0021	−0.0016
2.0	0.0107	0.0077	0.0062	0.0061	0.0060	−0.0117	−0.0093	−0.0064	−0.0064	−0.0066	−0.0009	0.0002	−0.0006	−0.0005	−0.0003
3.0	−0.0001	0.0002	0.0003	0.0003	0.0004	−0.0007	−0.0009	−0.0012	−0.0011	−0.0013	0.0003	0.0017	0.0002	0.0002	0.0002
4.0	−0.0005	−0.0005	−0.0005	−0.0005	−0.0005	0.0012	0.0013	0.0013	0.0012	0.0012	−0.0002	0.0002	−0.0002	−0.0001	−0.0001
5.0	−0.0000	0.0000	0.0000	0.0000	0.0000	−0.0001	0.0001	0.0001	0.0000	0.0000	0.0000	0.0000	0.0000	0.0000	0.0000
norm	5.000_5	5.000_4	5.000_4	5.000_4	5.000_4	5.000_4	5.000_3	5.000	5.000_3	5.007	5.000_5	5.000_4	5.000_3	5.000_4	5.000_3
$\langle \frac{1}{2}p_\theta^2 \rangle$	36.821_4	37.083_3	37.053_0	37.277_0	37.063_3	36.770_6	37.045_5	37.039_1	37.249_9	37.032_2	36.794_7	37.066_3	37.023_8	37.264_1	37.050_7

TABLE V. The isotropic Compton profile for the methane molecule.

q (a.u.)	SCF (6.3)	SCF (11.7)	SCF (11.7.1)	SDCI (11.7.1)	SCF (13.8.2)	SCF[a]	SDCI[b]	xr[c]	el[d]	el[e]
0.0	4.952	5.057	5.050	5.026	5.046	5.048	5.024	4.986	5.02	5.045
0.1	4.904	5.010	5.004	4.980	5.002	5.004	4.979	4.930	4.94	4.970
0.2	4.763	4.866	4.861	4.837	4.865	4.866	4.841	4.769	4.85	4.765
0.3	4.532	4.622	4.619	4.595	4.628	4.629	4.604	4.503	4.51	4.450
0.4	4.218	4.287	4.284	4.260	4.293	4.294	4.270	4.173	4.18	4.090
0.5	3.837	3.881	3.876	3.854	3.878	3.880	3.856	3.772	3.71	3.620
0.6	3.412	3.432	3.422	3.403	3.414	3.415	3.395	3.335	3.25	3.210
0.7	2.968	2.964	2.952	2.937	2.936	2.935	2.920	2.891	2.82	2.760
0.8	2.531	2.506	2.494	2.485	2.477	2.474	2.465	2.455	2.39	2.310
0.9	2.123	2.081	2.071	2.068	2.058	2.055	2.052	2.051	2.00	1.900
1.0	1.760	1.704	1.700	1.702	1.693	1.690	1.694	1.685	1.63	1.550
1.2	1.186	1.122	1.129	1.140	1.133	1.133	1.145	1.114	1.13	1.060
1.4	0.805	0.750	0.763	0.776	0.769	0.771	0.786	0.765	0.78	0.745
1.6	0.566	0.529	0.541	0.554	0.546	0.547	0.562	0.575	0.55	0.545
1.8	0.420	0.399	0.408	0.420	0.411	0.411	0.423	0.473	0.41	0.420
2.0	0.330	0.321	0.326	0.336	0.327	0.327	0.337	0.386	0.33	0.340
3.0	0.164	0.166	0.165	0.167	0.165	0.165	0.166		0.15	0.157
4.0	0.096	0.097	0.097	0.097	0.097	0.096	0.097		0.082	0.091
5.0	0.056	0.056	0.056	0.056	0.056	0.056	0.056		0.052	0.053

[a]Reference 16.
[b]Reference 15.
[c]Reference 42.
[d]Reference 41.
[e]Reference 40.

diffuse one-dimensional density.

The density in position space is intuitively understandable on the basis of the concept of hybrid orbitals,[38] i.e., sp^3 hybrids. The corresponding momentum density is different. The directional effect is only "half" visible in the sense that the density corresponds to that built up from an s and a p orbital independently. There is no contribution to the momentum density from a one-center orbital product in which the l quantum numbers differ by an odd integer.[39] This statement is only true under the assumption that the orbital coefficients, as in the present case, are real.[36]

With these additional rules of thumb one can understand that the plane through the origin orthogonal to direction 1 does in fact contain the largest amount of momentum density and thus the highest peak value of the DCP's is that of $J(0)$ in that direction. Similarly, the p-orbital contributions from the carbon towards each hydrogen give rise to momentum densities elongated along and opposite to the bond directions with a nodal plane through the origin. The DCP along a CH bond is thus expected to decay slowly, since there exist planes near to the origin and orthogonal to this direction which contain an appreciable amount of momentum density. For an illustration of a CH bond, the reader is referred to a momentum-density contour plot of this orbital, within the localized molecular orbital model, in the work by Epstein.[13]

In conclusion, we note that although the position and momentum densities are strongly related (especially for atoms), the methane molecule illustrates a case where the planes through the center of the molecule which contain the dominant electron density are different for position and for momentum space.

V. RESULTS AND DISCUSSION OF ISOTROPIC SCATTERING PROPERTIES

A. The isotropic Compton profiles

The calculated isotropic Compton profile for each of our five wave functions are included in Table V. The fluctuations in the profiles on improving the SCF wave functions beyond (11.7) are minor. At the peak, the trend is to lower the peak value, but already for $q=0.2$ a.u. any trend is lost. The largest changes occur not at the peak, but for $q=0.9$ a.u. where the SCF (13.8.2) function value is 0.029 (1.2%) lower than that from the SCF (11.7). Percentagewise, the difference reaches its maximum (3%) in the q range 1.6— 1.8 a.u.

Correlation effects are known to be of greater importance for certain systems.[6,34] The profile decreases with correlation for q less than 1.0 a.u. and increases in the region $1.0 \leqq q \leqq 2.0$ a.u. The decrease in the interval $0.0 \leqq q \leqq 0.4$ a.u. is constant (0.024) and is the largest absolute change found. The relative increase is largest in the region 1.2—2.0 a.u., where it is at most 3%. Although the carbon core orbitals were kept frozen in the SDCI calculation, the effect of core correlation should be small for smaller q.

The data published by Coulson and Duncanson[11] and by Epstein[13] do not allow a comparison with the ICP oth-

TABLE VI. The calculated isotropic Compton profile values for the methane molecule convoluted with the Helsinki residual instrumental function (RIF) and compared with the γ-ray experimental data (Ref. 43).

q (a.u.)	SCF (6.3)	SCF (11.7)	SCF (11.7.1)	SDCI (11.7.1)	SCF (13.8.2)	Expt. γ
0.0	4.927	5.036	5.032	5.006	5.037	4.899
0.1	4.877	4.984	4.979	4.953	4.983	4.842
0.2	4.731	4.828	4.823	4.798	4.826	4.685
0.3	4.496	4.579	4.573	4.549	4.574	4.438
0.4	4.187	4.251	4.244	4.222	4.243	4.116
0.5	3.820	3.863	3.855	3.836	3.851	3.739
0.6	3.416	3.436	3.428	3.411	3.422	3.327
0.7	2.994	2.993	2.985	2.972	2.977	2.903
0.8	2.574	2.553	2.546	2.538	2.539	2.487
0.9	2.174	2.136	2.131	2.128	2.124	2.096
1.0	1.807	1.757	1.755	1.756	1.749	1.744
1.2	1.206	1.145	1.149	1.158	1.148	1.178
1.4	0.796	0.740	0.749	0.763	0.753	0.798
1.6	0.547	0.506	0.518	0.532	0.523	0.568
1.8	0.407	0.384	0.394	0.406	0.398	0.436
2.0	0.327	0.318	0.324	0.334	0.326	0.360
3.0	0.163	0.165	0.164	0.166	0.164	0.190
4.0	0.096	0.097	0.097	0.097	0.097	0.108
5.0	0.056	0.056	0.056	0.056	0.056	0.057

TABLE VII. The isotropic $\overline{B}(r)$ function for the methane molecule.

r (a.u.)	SCF (6.3)	SCF (11.7)	SCF (11.7.1)	SDCI (11.7.1)	SCF (13.8.2)
0.00	10.000	10.000	10.000	10.000	10.000
0.04	9.976	9.978	9.979	9.979	9.979
0.10	9.872	9.873	9.873	9.872	9.873
0.20	9.550	9.549	9.550	9.547	9.550
0.30	9.123	9.124	9.125	9.119	9.125
0.40	8.661	8.668	8.669	8.658	8.668
0.50	8.206	8.219	8.219	8.204	8.218
0.60	7.776	7.794	7.794	7.773	7.791
0.70	7.371	7.397	7.395	7.369	7.391
0.80	6.989	7.024	7.020	6.989	7.016
0.90	6.624	6.671	6.664	6.629	6.659
1.00	6.272	6.332	6.322	6.283	6.317
1.20	5.596	5.681	5.667	5.621	5.661
1.40	4.947	5.056	5.036	4.988	5.030
1.60	4.319	4.450	4.427	4.379	4.422
1.80	3.721	3.868	3.845	3.799	3.840
2.00	3.160	3.318	3.296	3.255	3.293
2.50	1.975	2.127	2.117	2.092	2.118
3.00	1.127	1.242	1.246	1.236	1.254
3.50	0.580	0.647	0.661	0.662	0.675
4.00	0.256	0.286	0.302	0.308	0.318
4.50	0.083	0.090	0.101	0.109	0.115
5.00	0.001	−0.003	0.003	0.009	0.010
6.00	−0.036	−0.042	−0.046	−0.043	−0.052
7.00	−0.023	−0.027	−0.033	−0.032	−0.044
8.00	−0.010	−0.012	−0.017	−0.017	−0.027
9.00	−0.004	−0.006	−0.008	−0.008	−0.015
10.00	−0.001	−0.003	−0.004	−0.003	−0.007

er than that the latter found a peak value of 5.045 for his minimal basis STO calculations. Although the type of wave function employed by Smith and Whangbo[14] is the same and the energetical quality is very close to our SCF (11.7) (energy differs by only 0.007%), the profiles are quite different. Their profile is between 0.5% and 0.75% larger for q less than 0.5 a.u., lower (up to 3%) in the region $0.6 \leqq q \leqq 1.2$ a.u., and larger again out to $q = 2.0$ a.u. It is remarkable that the profiles have relative changes of up to 500 times that of the energy, when both of the wave functions are Gaussian-type basis orbital sets of almost the same "size."

Ahlenius and Lindner[15] presented only the profile from their SDCI wave function, which is very similar to that determined here. The largest deviations are in the region $0.7 \leqq q \leqq 0.9$ a.u., where their profile is nearly 1% higher than ours. Their SDCI and previously unpublished SCF results[16] are included in Table V.

Two Compton profile experiments[40,41] based on high-energy electron-impact spectroscopy (HEEIS) have recently been published for CH_4. There also exists an earlier x-ray experiment by Eisenberger and Marra[42] and a more recent γ-ray experiment due to Paakari and Merisalo.[43] A common discrepancy between all calculations and all experiments is that the latter give too low values in the region $0.3 \leqq q \leqq 1.0$ a.u. The x-ray experiment, performed before the multiple scattering problem was fully explored,[6] also gives too high values of $\bar{J}(q)$ for larger q values. This latter deviation is not found in the more recent (HEEIS) experiments. The profile reported by Klapthor and Lee[41] is slightly lower than that of Lahmam-Bennani *et al.*[40] at the peak, but most noticeable is the increase in the region $0.2 \leqq q \leqq 1.2$ a.u., i.e., an improvement towards a better agreement with theory, and where their differences are largest. The theoretical calculations which are close to experiment in this "crucial" region are pleasingly the two most sophisticated wave functions, the SDCI one due to Ahlenius and Lindner[15] and the SDCI one presented here. The SCF (13.8.2) is the best among the SCF wave functions in the outer part of this region ($q \geqq 0.6$ a.u.). We note that the (HEEIS) profiles are not normalized to the number of electrons as are our profiles and the γ-ray and x-ray data. Instead they satisfy the Bethe sum rule and their norm is slightly smaller than ten.

In order to have a meaningful comparison with the γ-ray experimental measurements,[43] we have convoluted our theoretical values for the Compton profile with the Helsinki[44] residual instrumental function (RIF). The resulting values of our Compton profiles are given in Table VI along with the γ-ray experimental data. Comparison of the data in Tables V and VI shows that there exists a discrepancy between the various experimental measurements and theoretical results in the region of low momenta ($0 < q < 1$ a.u.). The HEEIS measurements are in better agreement with the theoretical values, particularly the SCF (13.8.2) function.

The convergence towards the experimental results with improving wave functions is encouraging and tells us that much of the theory of the Compton scattering process is understood. But since there still is a region in which theory and experiment do not fit within the error bars, new experiments and further research in the fundamental process or the approximations employed need and ought to be made for a complete understanding of this inelastic scattering phenomenon.

B. Isotropic internally folded density [$B(\mathbf{r})$]

The isotropic component of the internally folded density (reciprocal form factor) $\bar{B}(r)$ has been obtained by means of Eq. (10) and the $\bar{B}(r)$ values calculated from the

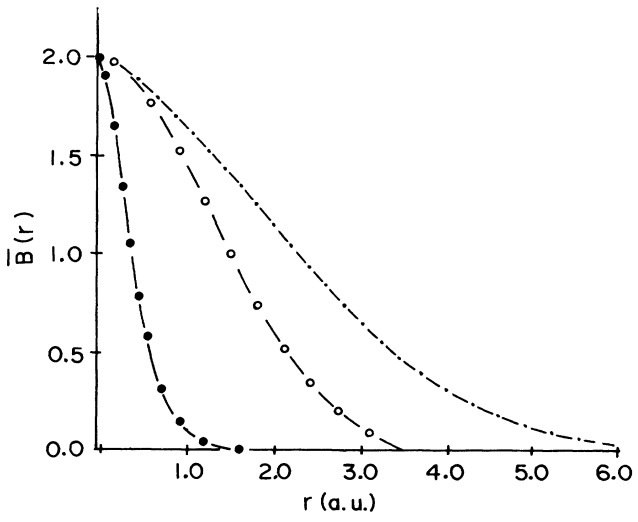

FIG. 2. Spherically averaged $\bar{B}(r)$ functions for individual orbitals: (i) —●— Core orbital ($1a_1$), (ii) —○— valence orbital ($2a_1$), (iii) —·—·—·— valence orbital ($1t_2$).

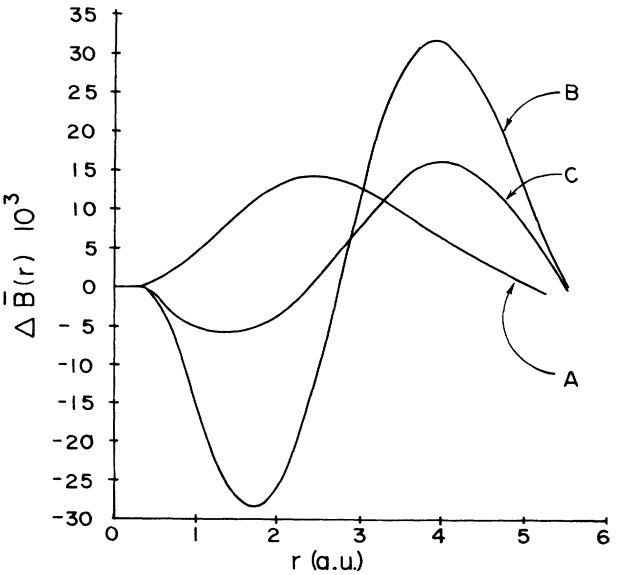

FIG. 3. Difference functions for $\bar{B}(r)$ for various SCF wave functions with respect to the (13.8.2): (a) (13.8.2)—(6.3) ($\times 10^{-1}$); (b) (13.8.2)—(11.7) ($\times 10^{-1}$); (c) 13.8.2—(11.7.1).

TABLE VIII. X-ray scattering intensities [Elastic (I_{el}^{xr}/I_T) and fully elastic (I_{fel}^{xr}/I_T)] for the methane molecule.

s (a.u.)	$\sin(\theta/\lambda)$ (Å^{-1})	I_{el}^{xr}/I_T SCF (6.3)	I_{fel}^{xr}/I_T SCF (6.3)	I_{el}^{xr}/I_T SCF (11.7)	I_{fel}^{xr}/I_T SCF (11.7)	I_{el}^{xr}/I_T SCF (11.7.1)	I_{fel}^{xr}/I_T SCF (11.7.1)	I_{el}^{xr}/I_T SDCI (11.7.1)	I_{fel}^{xr}/I_T SDCI (11.7.1)	I_{el}^{xr}/I_T SCF (13.8.2)	I_{fel}^{xr}/I_T SCF (13.8.2)
0.00	0.00	100.000	100.000	100.000	100.000	100.000	100.000	100.000	100.000	100.000	100.000
0.067	0.01	99.492	99.492	99.468	99.468	99.472	99.472	99.471	99.471	99.473	99.473
0.133	0.02	97.986	97.986	97.892	97.892	97.907	97.907	97.904	97.904	97.910	97.910
0.266	0.04	92.213	92.213	91.874	91.874	91.928	91.928	91.919	91.919	91.940	91.940
0.399	0.06	83.430	83.428	82.778	82.776	82.888	82.887	82.875	82.874	82.914	82.913
0.532	0.08	72.692	72.686	71.758	71.753	71.931	71.926	71.923	71.917	71.974	71.969
0.665	0.10	61.150	61.131	60.038	60.019	60.269	60.252	60.277	60.259	60.330	60.313
0.798	0.12	49.838	49.792	48.681	48.637	48.959	48.916	48.991	48.948	49.034	48.992
0.931	0.14	39.535	39.443	38.458	38.369	38.761	38.675	38.823	38.737	38.843	38.760
1.064	0.16	30.707	30.548	29.797	29.646	30.099	29.953	30.192	30.045	30.180	30.037
1.197	0.18	23.523	23.281	22.821	22.595	23.098	22.878	23.216	22.996	23.169	22.953
1.330	0.20	17.924	17.591	17.433	17.127	17.666	17.366	17.802	17.503	17.722	17.426
1.463	0.22	13.713	13.294	13.405	13.027	13.586	13.211	13.730	13.357	13.627	13.253
1.596	0.24	10.630	10.140	10.468	10.035	10.593	10.158	10.739	10.307	10.622	10.185
1.729	0.26	8.4127	7.8788	8.3582	7.8936	8.4325	7.9584	8.5743	8.1050	8.4548	7.9741
1.862	0.28	6.8333	6.2851	6.8533	6.3841	6.8855	6.3972	7.0192	6.5377	6.9044	6.4058
1.995	0.30	5.7094	5.1768	5.7798	5.3308	5.7790	5.3009	5.9026	5.4330	5.7972	5.3061
2.660	0.40	3.3659	3.1379	3.5202	3.3380	3.4557	3.2292	3.5261	3.3092	3.4715	3.2348
3.325	0.50	2.7915	2.7459	2.9066	2.8705	2.8684	2.8213	2.8976	2.8530	2.8658	2.8152
3.990	0.60	2.4106	2.3936	2.4589	2.4450	2.4582	2.4450	2.4639	2.4507	2.4492	2.4356
4.655	0.70	2.0239	2.0168	2.0393	2.0337	2.0458	2.0404	2.0443	2.0389	2.0414	2.0359
5.320	0.80	1.7096	1.7071	1.7171	1.7151	1.7192	1.7172	1.7172	1.7151	1.7166	1.7147
5.985	0.90	1.4529	1.4516	1.4590	1.4579	1.4586	1.4575	1.4573	1.4561	1.4570	1.4559
6.650	1.00	1.2150	1.2145	1.2209	1.2205	1.2200	1.2196	1.2192	1.2188	1.2198	1.2194
7.980	1.20	0.808 36	0.808 31	0.809 69	0.809 56	0.808 51	0.808 39	0.808 36	0.808 24	0.809 59	0.809 48
9.310	1.40	0.523 47	0.523 47	0.525 12	0.525 08	0.524 01	0.523 98	0.524 22	0.524 18	0.524 47	0.524 44
10.640	1.60	0.331 36	0.331 36	0.334 60	0.334 59	0.333 86	0.333 85	0.334 11	0.334 09	0.333 76	0.333 75
11.970	1.80	0.207 63	0.207 63	0.212 11	0.212 11	0.211 66	0.211 63	0.211 84	0.211 84	0.211 36	0.211 35
13.299	2.00	0.130 06	0.130 06	0.134 88	0.134 88	0.134 60	0.134 59	0.134 75	0.134 75	0.134 38	0.134 38
15.960	2.40	0.052 606	0.052 606	0.055 669	0.055 669	0.055 572	0.055 571	0.055 638	0.055 638	0.055 533	0.055 533
18.620	2.80	0.022 798	0.022 798	0.024 046	0.024 046	0.024 014	0.024 013	0.024 041	0.024 041	0.024 039	0.024 039
19.950	3.00	0.015 384	0.015 384	0.016 109	0.016 109	0.016 089	0.016 089	0.016 107	0.016 107	0.016 124	0.016 124
26.599	4.00	0.002 310	0.002 310	0.002 655	0.002 655	0.002 652	0.002 652	0.002 655	0.002 655	0.002 655	0.002 655
33.249	5.00	0.000 291	0.000 291	0.000 578	0.000 578	0.000 577	0.000 577	0.000 578	0.000 578	0.000 576	0.000 576

various SCF and SDCI functions are reported in Table VII. It is seen from the table that the $\overline{B}(r)$ functions decrease monotonically with r and cross the axis at $r \approx 5$ ("zero passage"[9]) and become negative. In Fig. 2 the $\overline{B}(r)$ functions for the individual occupied molecular orbitals of CH_4 are displayed. It is seen that the contribution due to the core orbital ($1a_1$) drops out very rapidly so that only the valence orbitals dominate the $\overline{B}(r)$ function beyond 1.7 a.u. This feature clearly shows that the valence electrons do not interfere with the core electrons. We have also looked into the basis set effect on the $\overline{B}(r)$ function. The differences of $\overline{B}(r)$ between the SCF (13.8.2) and the SCF (6.3), SCF (11.7), and SCF (11.7.1) functions are shown in Fig. 3. It is noticed that the $\overline{B}(r)$ function is sensitive to the inclusion of polarization functions, particularly between $1 \leqq r \leqq 5$.

C. Isotropic scattering factors

The spherically averaged elastic and fully elastic x-ray intensities were obtained from Eqs. (3) and (4), respectively, by carrying out a numerical integration over the scattering angles. The calculated values of the intensities using the various wave functions involving different degrees of sophistication, as described in Sec. II, are given in Table VIII. The scattering of a particle is usually described in terms of the scattering parameter s defined by $4\pi \sin\theta/\lambda$, where 2θ is the scattering angle and λ is the wavelength of the incident radiation. Since it has been already seen in the case of directional scattering factors (Sec. III A) that there is hardly any dependence on the quality of the wave function, it is not surprising that a similar trend exists also for the isotropic component of the elastic and fully elastic intensities. It is clearly seen from Table VIII that $I_{\rm el}^{\rm xr}(s)/I_T$ is always greater than $I_{\rm fel}^{\rm xr}(s)/I_T$ in accordance with Eq. (5). The maximum deviation of 7% occurs near $\sin(\theta/\lambda) \approx 0.28$ Å^{-1}. This small difference observed between $I_{\rm el}^{\rm xr}/I_T$ and $I_{\rm fel}^{\rm xr}(s)/I_T$ is basically due to the very weak anisotropy of the CH_4 molecule.

ACKNOWLEDGMENTS

This work was supported by the Natural Sciences and Engineering Research Council of Canada (NSERCC). We wish to thank Dr. P. Lindner for permitting us to use the previously unpublished SCF results of Ahlenius and Lindner for the isotropic Compton profile.

*Permanent address: Department of Physics, University of Roorkee, Roorkee 247667, India.

[1]R. Benesch and V. H. Smith, Jr., in *Wave Mechanics—the First Fifty Years,* edited by W. C. Price *et al.* (Butterworths, London, 1973), pp. 357—377; Acta Crystallogr., Sect. A **26**, 579 (1970).

[2]R. A. Bonham and M. Fink, *High Energy Electron Scattering* (Van Nostrand Reinhold, New York, 1974).

[3]W. Kolos, H. J. Monkhorst, and K. Szalewicz, J. Chem. Phys. **77**, 1323 (1982).

[4]A. J. Thakkar, A. N. Tripathi, and V. H. Smith, Jr., Phys. Rev. A **29**, 1108 (1984).

[5]A. N. Tripathi and V. H. Smith, Jr., in *Comparison of Ab Initio Quantum Chemistry with Experiment: State-of-the-Art,* edited by R. Bartlett (Reidel, Dordrecht, 1985), pp. 439—462, and references therein.

[6]*Compton Scattering: The Investigation of Electron Momentum Distributions,* edited by B. G. Williams (McGraw-Hill, London, 1977).

[7]P. Kaijser and V. H. Smith, Jr., Adv. Quantum Chem. **10**, 37 (1977).

[8]R. Benesch, S. R. Singh, and V. H. Smith, Jr., Chem. Phys. Lett. **10**, 151 (1971).

[9]W. Weyrich, P. Pattison, and B. G. Williams, Chem. Phys. **41**, 271 (1979).

[10]A. J. Thakkar, A. M. Simas, and V. H. Smith, Jr., Chem. Phys. **63**, 175 (1981).

[11]W. E. Duncanson and C. A. Coulson, Proc. Cambridge Philos. Soc. **37**, 406 (1941); C. A. Coulson and W. E. Duncanson, *ibid.* **38**, 100 (1941).

[12]M. Cornille, M. Roux, and B. Tsapline, Acta Crystallogr., Sect. A **26**, 105 (1970).

[13]I. R. Epstein, J. Chem. Phys. **53**, 4425 (1970).

[14]V. H. Smith, Jr. and M. H. Whangbo, Chem. Phys. **5**, 234 (1974); M. H. Whangbo, V. H. Smith, Jr., and W. von Niessen, *ibid.* **6**, 282 (1974).

[15]T. Ahlenius and P. Lindner, Chem. Phys. Lett. **34**, 123 (1975); J. Phys. B **8**, 778 (1975).

[16]T. Ahlenius and P. Lindner (private communication).

[17]M. T. Cooper, Rep. Prog. Phys. **48**, 415 (1985).

[18]B. G. Williams and J. M. Thomas, Int. Rev. Phys. Chem. **3**, 39 (1983).

[19]R. McWeeny, Acta Crystallogr. **6**, 631 (1953).

[20]P. Kaijser, A. N. Tripathi, V. H. Smith, Jr., and G. H. F. Diercksen (unpublished).

[21]D. G. Whiffen, Pure Appl. Chem. **50**, 75 (1978).

[22]G. H. F. Diercksen and W. P. Kramer, MUNICH, Molecular Program System—Reference Manual, Special Report, Max-Planck-Institut für Physik und Astrophysik, München, 1973 (unpublished).

[23]C. Salez and A. Veillard, Theor. Chim. Acta **11**, 441 (1968); S. Huzinaga, J. Chem. Phys. **42**, 1293 (1965).

[24]F. B. von Duijnefeldt, IBM Research Report No. RJ945, 1971 (unpublished); E. Clementi and H. Popkie, J. Am. Chem. Soc. **94**, 4066 (1972).

[25]W. J. Hehre, R. F. Stewart, and J. A. Pople, J. Chem. Phys. **51**, 2657 (1969).

[26]The CI program is taken from the program system MOLECULE, developed at Stockholm University and adapted to the system MUNICH. It is described in B. Roos, Chem. Phys. Lett. **15**, 153 (1972). The program for transforming the two-electron integrals is described in G. H. F. Diercksen, Theor. Chim. Acta **33**, 1 (1974).

[27]D. R. J. Boyd and H. W. Thompson, Trans. Faraday Soc. **49**, 1281 (1953).

[28]A. M. Simas, A. J. Thakkar, and V. H. Smith, Jr., Int. J. Quantum Chem. **21**, 419 (1982); **24**, 527 (1983).

[29]J. Kowaleski, B. Roos, P. Siegbahn, and R. Vestin, Chem. Phys. **9**, 29 (1975).

[30]R. M. Pitzer, J. Chem. Phys. **46**, 4871 (1967).

[31]P.-O. Löwdin, J. Mol. Spectrosc. **3**, 40 (1959).
[32]A. Farazdel, W. M. Westgate, A. M. Simas, R. P. Sagar, and V. H. Smith, Jr., Int. J. Quantum Chem. **S19**, 61 (1985).
[33]P. Kaijser and P. Lindner, Philos. Mag. **31**, 871 (1975).
[34]R. Benesch and V. H. Smith, Jr., Phys. Rev. A **5**, 114 (1972) R. E. Brown and V. H. Smith, Jr., *ibid.* **5**, 140 (1972); V. H Smith, Jr., and R. E. Brown, Chem. Phys. Lett. **20**, 424 (1973); R. E. Brown and V. H. Smith, Jr., Mol. Phys. **34**, 713 (1977).
[35]A. Tanner and I. R. Epstein, Chap. 5 in Ref. 6.
[36]P. Kaijser and V. H. Smith, Jr., in *Quantum Science: Methods and Structure*, edited by J.-L. Calais *et al.* (Plenum, New York, 1976), p. 417.
[37]W. J. Janis, P. Kaijser, J. R. Sabin, and V. H. Smith, Jr., Mol. Phys. **37**, 463 (1978); W. J. Janis, P. Kaijser, V. H. Smith, Jr., and M. H. Whangbo, *ibid.* **35**, 1237 (1978); P. Kaijser, V. H. Smith, Jr., and A. J. Thakkar, *ibid.* **41**, 1143 (1980).
[38]C. A. Coulson, *Valence* (University Press, Oxford, 1952).
[39]P. Kaijser and V. H. Smith, Jr., Mol. Phys. **31**, 1557 (1976).
[40]A. Lahmam-Bennani, H. F. Wellenstein, A. Duguet, B. Nguyen, and A. D. Barlas, Chem. Phys. Lett. **41**, 470 (1976).
[41]R. W. Klapthor and J. S. Lee, Chem. Phys. Lett. **45**, 513 (1977).
[42]P. Eisenberger and W. C. Marra, Phys. Rev. Lett. **27**, 1413 (1971).
[43]T. Paakari and M. Merisalo, Chem. Phys. Lett. **53**, 313 (1978).
[44]P. Paatero, S. Manninen, and T. Paakari, Philos. Mag. **30**, 1281 (1974).